Tanzania Journal of Science 50(3): 692-712, 2024
ISSN 0856-1761, e-ISSN 2507-7961

An Age-Structured Model for the Effects of Temperature and Rainfall on the Transmission Dynamics of Malaria

Alanus Mapunda[1*], Eunice Mureithi[1] and Nyimvua Shaban[1],
[1]*Department of Mathematics, University of Dar es Salaam, P.O. Box 35062, Dar es Salaam, Tanzania*
Emails: ewambui02@gmail.com, shabanmbare@gmail.com
[*]*Corresponding author: alanusmapunda9@gmail.com*
Received 17 Apr 2024, Revised 20 Aug 2024, Accepted 26 Sep 2024, Publ. 30 Sept. 2024
https://dx.doi.org/10.4314/tjs.v50i3.22

Abstract

This study has investigated the impact of temperature and rainfall on the transmission dynamics of malaria using an age-structured population model, with a class of pregnant women. The equilibrium solutions have been analyzed, and numerical simulations carried out. The results show that there are significantly high rates of malaria infections for the temperature and rainfall ranging between ($23.53\ ^0C - 39.80\ ^0C$) and (14.82 mm − 38.44 mm) respectively. The results have shown that, the most affected populations are children up to five years old and pregnant women, and that decreasing the rate of transplacental transmission increases the number of children born free of malaria infections. Therefore, this work recommends human individuals to be aware of the variations of temperature, rainfall, and their corresponding ranges at which malaria transmission occurs most, so that they can take precautions.

Keywords: Age-structure; Pregnant women; Temperature and rainfall; Malaria dynamics; Transplacental transmission.

Introduction

Malaria is a mosquito-borne disease caused by parasites of the genus plasmodium. The parasites are of five species namely; *Plasmodium falciparum*, *plasmodium vivax*, *plasmodium knowlesi*, *plasmodium ovale* and *plasmodium malariae*. *Plasmodium falciparum* and *plasmodium vivax* are the most virulent and potentially lethal to humans (Yang 2000). Malaria parasites are transmitted to human via the bites of infectious female anopheles mosquitoes. An infected human can experience fever, headache, vomiting, stomachache and sometimes diarrhea. Another way in which malaria can be transmitted is from an infected pregnant mother to a baby before or during delivery (Kipkirui et al. 2020).

In areas with high rates of malaria transmission, pregnant women and children up to five years represent the most vulnerable groups to malaria infections (Bakary et al. 2018). High rates of malaria infections during pregnancy can cause transplacental transmission of the malaria parasites to the foetus (Uneke 2011, Ou´edraogo et al. 2012, Schumacher and Spinelli 2012). This situation increases the rate of maternal morbidity and mortality, high fever, severe anemia, miscarriage and stillbirth (Uneke 2011). Moreover, Malaria infections in children under five years, increase the risk of morbidity and mortality for the children as they have not yet developed sufficient immunity to fight against malaria (Schumacher and Spinelli 2012). However, it is realized that in areas of low and unstable transmission, people of all groups are at risk of malaria infections (Schumacher and Spinelli 2012).

The dynamics of malaria are influenced by some non-weather and weather factors. Non-weather factors include population movements, urbanization and interruption of

control and preventive measures, capacity of health care systems, herd immunity and social behavior of the population (Kumar and Reddy 2014, Bakare and Abolarin 2018). Floods, droughts, temperature, rainfall or relative humidity are weather conditions that influence parasites life cycle (Kumar and Reddy 2014).

According to estimates by World Health Organization (WHO), there were 229 million new malaria cases and 409,000 deaths due to malaria in 2019 globally. Moreover, 67% of these mortality cases being among children under five years of age, and 822,000 children born with low weight. Furthermore, in the year 2020, there were 241 million new malaria cases and 627,000 deaths due to the disease worldwide (World malaria report 2022). Likewise, in 2021 the estimates showed 247 million new malaria cases and 619,000 mortality cases globally. In addition, 95% of these cases were from Africa; infants, children under five years and pregnant women were the most affected than other human individuals (World malaria report 2023). In Tanzania, malaria burden in some of the regions is still high. The study conducted by Mwaiswelo et al. (2021) in Mtwara region reported 15.9% prevalence in 2340 children and 53.9% anemia in 2218 children. They also mentioned that education and socioeconomic were sources of the infections.

Different studies have been extensively conducted to explore the effects of climatic change on the dynamics of malaria and measures that can be taken to prevent its devastating effect on human population as pointed out by studies of Blanford et al. (2013), Ngarakana-Gwasira et al. (2016), Gumel and Okuneye (2017), Bakare and Abolarin (2018), Abiodun et al. (2018), Azu-Tungmah et al. (2019) and Yiga et al. (2020). The work by, Azu-Tungmah et al. (2019) proposed an age-structured mathematical malaria model incorporating pregnant women. However, in their work, transplacental transmission, temperature and rainfall were not considered. In particular, the work by Gumel and Okuneye (2017) explored the effect of temperature and rainfall in malaria transmission dynamics for an age-structured human and mosquito populations. Nevertheless, in their work, pregnant women and transplacental transmission were not considered. Thus, this study intends to investigate the transmission dynamics of malaria infections in pregnant women, transplacental transmission of infection to the new born child, age-structured human population, and the influence of temperature and rainfall on the survival and biting rate of the malaria causing female anopheles mosquitoes.

Materials and Methods

The Model

A basic mathematical model for malaria that is considered here comprises of mosquito population $N_v(t)$ and human population $N_h(t)$. The human population is divided into the sub-populations of pregnant women, children up to five years old and individuals above five years old (excluding pregnant women). The sub-populations are further sub-divided into susceptible S_i and infected, I_i groups for $i = p, c, a$, where p represents pregnant women, c stands for children up to five years old and a denotes individuals above five years old (excluding pregnant women), and they all recover to the R_h (t). The total size of mosquito and human populations at any time $t > 0$ is given by $N_v(t) = S_v(t) + I_v(t)$ and $N_h(t) = S_p(t) + S_c(t) + S_a(t) + I_p(t) + I_c(t) + I_a(t) +$ respectively. We assume that the rate at which individuals are recruited by immigration into the susceptible class of over five years old is π_a. The rate at which women become pregnant is α_1, while susceptible children up to five years are recruited by birth from either susceptible pregnant women at a rate β_p or from infected pregnant women at a rate $\beta(1-\alpha)$.

All susceptible human individuals become infected after being bitten by infectious mosquitoes, according to the force of infection; $\lambda_i(t;T) = b(T)\gamma_i \frac{I_v(t)}{N_h(t)}$ for $i = p, c, a$, and with usual notation of p, c and a. Here γ_i is the probability that mosquito bite transmits malaria parasites, and $b(T)$ is the mosquito temperature-dependent biting rate.

We assume that all infected human individuals recover naturally and join the class R_h(t) at the rates σ_p, σ_c and σ_a for pregnant women, children up to five years old and individuals above five years (excluding pregnant women) respectively. A susceptible pregnant woman in S_p can deliver a baby and join the class S_a at the rate α_2. The susceptible child can grow and join the susceptible class S_a at the rate β_s. Similarly, an infectious pregnant I_p can give birth to a baby and join infectious I_a at the rate σ_2. Also, an infectious adult woman from I_a can become pregnant and join the class, I_p at σ_1. An infectious child in I_c can grow and join the infectious class of individuals above five years, I_a at the rate β_c. It is supposed that a fraction of children is born with malaria parasites. It is assumed that β is a total rate at which babies are born from infected pregnant women. The possibility that a baby delivered by an infectious pregnant woman is infected is $\alpha \in [0,1]$ (that is, $\beta\alpha$ is the fraction of babies born with malaria infections). All human individuals experience natural death at the per capita rate μ_h. Infected individuals suffer from the malaria induced death rates μ_p, μ_c and μ_a for pregnant women, children up to five years and those above five years respectively. Mosquitoes are recruited into the susceptible class S_v, by birth at a temperature-rainfall dependent per capita birth rate of $\eta(T, R_m)$. A susceptible mosquito becomes infected based on a force of infection; $\lambda_v(t;T) = b(T)\gamma_v \frac{1}{N_h(t)}\left(I_p(t) + I_c(t) + I_a(t)\right)$, with γ_v being the probability at which a mosquito gets infected. Mosquitoes leave the population through natural death at a rate μ_v. Figure 1 shows a schematic presentation of the transmission dynamics of malaria for a population with age-structure and pregnant women.

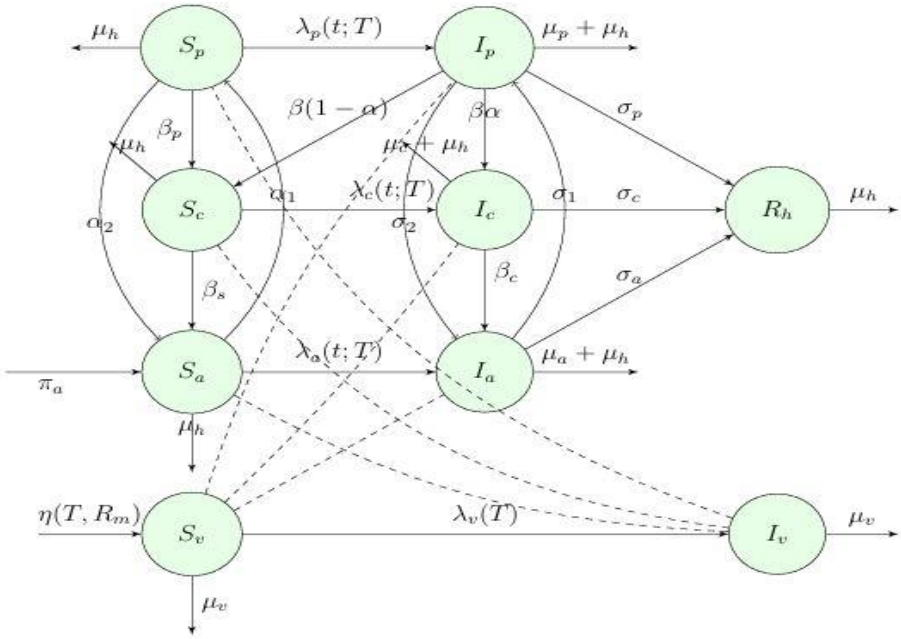

Figure 1: Schematic presentation of the transmission dynamics of malaria for a population with age-structure and pregnant women

Model Equations

$$
\begin{aligned}
\frac{dS_p}{dt} &= \alpha_1 S_a - (\lambda_p(t;T) + \beta_p + \alpha_2 + \mu_h)S_p,\\
\frac{dS_c}{dt} &= \beta(1-\alpha)I_p + \beta_p S_p - (\lambda_c(t;T) + \beta_s + \mu_h)S_c,\\
\frac{dS_a}{dt} &= \pi_a + \beta_s S_c + \alpha_2 S_p - (\lambda_a(t;T) + \alpha_1 + \mu_h)S_a,\\
\frac{dI_p}{dt} &= \lambda_p(t;T)S_p + \sigma_1 I_a - (\sigma_2 + \sigma_p + \beta + \mu_p + \mu_h)I_p,\\
\frac{dI_c}{dt} &= \lambda_c(t;T)S_c + \beta\alpha I_p - (\sigma_c + \beta_c + \mu_c + \mu_h)I_c,\\
\frac{dI_a}{dt} &= \lambda_a(t;T)S_a + \sigma_2 I_p + \beta_c I_c - (\sigma_1 + \sigma_a + \mu_a + \mu_h)I_a,\\
\frac{dR_h}{dt} &= \sigma_p I_p + \sigma_c I_c + \sigma_a I_a - \mu_h R_h,\\
\frac{dS_v}{dt} &= \eta(T, R_m) - (\lambda_v(t;T) + \mu_v(T))S_v,\\
\frac{dI_v}{dt} &= \lambda_v(t;T)S_v - \mu_v(T)I_v.
\end{aligned}
\tag{2.1}
$$

The initial conditions of model system (2.1) are $S_p(0) > 0$, $S_c(0) > 0$, $S_a(0) > 0$, $I_p(0) \geq 0$, $I_c(0) \geq 0$, $I_a(0) \geq 0$, $R_h(0) \geq 0$, $S_v(0) > 0$, $I_v(0) \geq 0$.

Invariant region

The model (2.1) is biologically meaningful in the invariant region $\Omega = \Omega_h \times \Omega_v$ where

$$\Omega_h = \left\{ S_p, S_c, S_a, I_p, I_c, I_a, R_h > 0 : S_p + S_c + S_a + I_p + I_c + I_a + R_h \leq \frac{\pi_a}{\mu_h} \right\}$$

and $\Omega_v = \left\{ S_v, I_v > 0 : S_v + I_v \leq \frac{\eta(T,R_m)}{\mu_v} \right\}$ is any solution of the system of equations in (2.1) and with all variables non-negative. So; $N_h \leq \frac{\pi_a}{\mu_h}$ and $N_v \leq \frac{\eta(T,R_m)}{\mu_v}$.

Therefore, the solution for human and mosquito populations enter the invariant region Ω. This means that the region is bounded and attracts all solutions of (2.1) in it. Thus, the solutions of model system (2.1) are positive and bounded for all $t > 0$.

Disease-Free Equilibrium and its Stability

Disease free equilibrium (DFE) is the steady state solution where there is no disease in the population. The disease will not exist in the two populations if the classes $I_p = I_c = I_a = I_v = 0$. The disease-free equilibrium of the model system (2.1) is given by

$$E_0 = \left(S_p^*, S_c^*, S_a^*, 0, 0, 0, 0, S_v^*, 0 \right) \quad , \quad (2.2)$$

where,

$$S_p^* = \frac{\alpha_1(\beta_s + \mu_h)\pi_a}{(\beta_s + \mu_h)(\alpha_1 + \mu_h)(\beta_p + \alpha_2 + \mu_h) - \alpha_1(\beta_s\beta_p + \alpha_2(\beta_s + \mu_h))},$$

$$S_c^* = \frac{\beta_p\alpha_1(\beta_s + \mu_h)\pi_a}{(\beta_s + \mu_h)\left[(\beta_s + \mu_h)(\alpha_1 + \mu_h)(\beta_p + \alpha_2 + \mu_h) - \alpha_1(\beta_s\beta_p + \alpha_2(\beta_s + \mu_h))\right]},$$

$$S_a^* = \frac{(\beta_p + \alpha_2 + \mu_h)(\beta_s + \mu_h)\pi_a}{(\beta_s + \mu_h)\left[(\beta_s + \mu_h)(\alpha_1 + \mu_h)(\beta_p + \alpha_2 + \mu_h) - \alpha_1(\beta_s\beta_p + \alpha_2(\beta_s + \mu_h))\right]} \text{ and } S_v^* = \frac{\eta(T,R_m)}{\mu_v(T)}.$$

The stability of E_0 is governed by the basic reproduction number. The reproduction number is evaluated using the next generation matrix method as below.

Reproduction Number

The basic reproduction number denoted by R_0 , is the expected number of secondary infections produced by a single infected individual in a susceptible population during the entire period of infectiousness. So, in order to investigate stability of E_0 we need to compute the basic reproduction number R_0 . Here, the next generation matrix technique is used, where R_0 is obtained by taking the largest eigenvalue (spectral radius) of the matrix $FV^{-1} = \left[\partial f_i(E_0) \big/ \partial x_j \right] \left[\partial v_i(E_0) \big/ \partial x_j \right]^{-1}$. Here f_i is the rate of appearance of new infections in compartment i , and v_i is the transfer of infections from one compartment to

another and E_0 is the DFE given in equation (2.2). From model system (2.1), we write the equations with infections classes I_p, I_c, I_a and I_v, which results into the following system

$$\frac{dI_p}{dt} = \lambda_p(t;T)S_p + \sigma_1 I_a - (\sigma_2 + \sigma_p + \beta + \mu_p + \mu_h)I_p,$$

$$\frac{dI_c}{dt} = \lambda_c(t;T)S_c + \beta\alpha I_p - (\sigma_c + \beta_c + \mu_c + \mu_h)I_c,$$

$$\frac{dI_a}{dt} = \lambda_a(t;T)S_a + \sigma_2 I_p + \beta_c I_c - (\sigma_1 + \sigma_a + \mu_a + \mu_h)I_a,$$

$$\frac{dI_v}{dt} = \lambda_v(t;T)S_v - \mu_v(T)I_v.$$

Using the notations in Van den Driessche and Watmough (2002), the matrices *F* and *V* for the new infections' terms and the remaining terms of equation (2.1) are respectively, given by

$$F = \begin{pmatrix} 0 & 0 & 0 & \frac{b\gamma_p S_p^*}{S_p^* + S_c^* + S_a^*} \\ 0 & 0 & 0 & \frac{b\gamma_c S_c^*}{S_p^* + S_c^* + S_a^*} \\ 0 & 0 & 0 & \frac{b\gamma_a S_a^*}{S_p^* + S_c^* + S_a^*} \\ \frac{b\gamma_v S_v^*}{S_p^* + S_c^* + S_a^*} & \frac{b\gamma_v S_v^*}{S_p^* + S_c^* + S_a^*} & \frac{b\gamma_v S_v^*}{S_p^* + S_c^* + S_a^*} & 0 \end{pmatrix}$$

and

$$V = \begin{pmatrix} \sigma_p + \sigma_2 + \beta + \mu_p + \mu_h & 0 & -\sigma_1 & 0 \\ -\beta\alpha & \sigma_c + \beta_c + \mu_c + \mu_h & 0 & 0 \\ -\sigma_2 & -\beta_c & \sigma_a + \sigma_1 + \mu_a + \mu_h & 0 \\ 0 & 0 & 0 & \mu_v \end{pmatrix}.$$

Thus, the reproduction number is the largest (dominant) eigenvalue (spectral radius) of the next generation matrix FV^{-1}. Hence,

$$R_0 = \rho\left(FV^{-1}\right) = \frac{b(T)}{\left(S_p^* + S_c^* + S_a^*\right)\mu_v R_1}\sqrt{\gamma_v \mu_v S_v^* \left(\gamma_p R_p S_p^* + \gamma_c R_c S_c^* + \gamma_a R_a S_a^*\right) R_1},$$

where

ρ is the spectral radius and

$$R_p = -\alpha\beta\sigma_a - \alpha\beta\sigma_1 + \beta\sigma_a + \beta_c\left(-\alpha\beta + \mu_a + \sigma_a + \beta + \mu_h + \sigma_1 + \sigma_2\right) + \mu_a(-\alpha\beta + \beta + \mu_c + \sigma_c + \mu_h) + \sigma_c(\sigma_a + \sigma_1 + \sigma_2 + \mu_h) + \sigma_a\mu_c + \beta\sigma_1 + \mu_c\mu_h + \sigma_1\mu_c + \sigma_2\mu_c - \alpha\beta\mu_h + \beta\mu_h + \sigma_1\mu_h + \sigma_2\mu_h + \mu_h^2,$$

$$R_c = \beta\sigma_a + \sigma_a\mu_h + \mu_a(\beta + \mu_h + \mu_p + \sigma_p + \sigma_2) + \sigma_p(\sigma_a + \mu_h + \sigma_1) + \sigma_a\mu_p + \sigma_2\sigma_a + \beta\sigma_1 + \beta_c(\beta + \mu_h + \mu_p + \sigma_p + \sigma_1 + \sigma_2) + \beta\mu_h + \sigma_1\mu_h + \sigma_2\mu_h + \mu_h^2 + \mu_p\mu_h + \sigma_1\mu_p,$$

$$R_a = -\alpha\beta\sigma_1 + \beta\sigma_1 + \beta\sigma_c + \sigma_c\mu_h + \beta_c(\beta + \mu_h + \mu_p + \sigma_p + \sigma_1 + \sigma_2) + \mu_c(\beta + \mu_h + \mu_p + \sigma_p + \sigma_1 + \sigma_2) + \sigma_p(\sigma_c + \mu_h) + \sigma_c\mu_p + \sigma_1\sigma_c + \sigma_2\sigma_c + \beta\mu_h + \sigma_1\mu_h + \sigma_2\mu_h + \mu_h^2 + \mu_p\mu_h,$$

$$R_1 = \beta_c(\alpha\beta\sigma_1 + \beta\sigma_a + \mu_h R_2 + \mu_a R_3 + \sigma_a\mu_p + \sigma_p(\sigma_a + \sigma_1) + \sigma_2\sigma_a + \mu_h^2 + \sigma_1\mu_p) + \left(\mu_c + \sigma_c + \mu_h\right)\left(\beta\sigma_a + \mu_h R_2 + \mu_a R_3 + \sigma_a\mu_p + \sigma_p\left(\sigma_a + \sigma_1\right) + \sigma_2\sigma_a + \beta\sigma_1 + \mu_h^2 + \sigma_1\mu_p\right),$$

$R_2 = \beta + \mu_p + \sigma_1 + \sigma_2 + \sigma_a + \sigma_p$ and $R_3 = \beta + \mu_h + \mu_p + \sigma_2 + \sigma_p$.

Thus, the effect of temperature and rainfall on the reproduction number R_0, is in S_v^* and biting rate $b(T)$ of mosquito.

Local Stability of the Disease-Free Equilibrium

Here we establish the stability of the DFE that is obtained in equation (2.2).

Theorem 1. *The disease-free equilibrium of model (2.1) is a locally asymptotically stable if* $R_0 < 1$ *and unstable otherwise.*

Proof:

We evaluate the Jacobian matrix at the disease-free equilibrium to get

$$J(E_0)=\begin{pmatrix} -D_1 & 0 & \alpha_1 & 0 & 0 & 0 & 0 & 0 & -b\gamma_p \frac{S_p^*}{N_h^*} \\ \beta_p & -D_2 & 0 & \beta(1-\alpha) & 0 & 0 & 0 & 0 & -b\gamma_c \frac{S_c^*}{N_h^*} \\ \alpha_2 & \beta_s & -D_3 & 0 & 0 & 0 & 0 & 0 & -b\gamma_a \frac{S_a^*}{N_h^*} \\ 0 & 0 & 0 & -D_4 & 0 & \sigma_1 & 0 & 0 & b\gamma_p \frac{S_p^*}{N_h^*} \\ 0 & 0 & 0 & \beta\alpha & -D_5 & 0 & 0 & 0 & b\gamma_c \frac{S_c^*}{N_h^*} \\ 0 & 0 & 0 & \sigma_2 & \beta_c & -D_6 & 0 & 0 & b\gamma_a \frac{S_a^*}{N_h^*} \\ 0 & 0 & 0 & \sigma_p & \sigma_c & \sigma_a & -\mu_h & 0 & 0 \\ 0 & 0 & 0 & -b\gamma_v \frac{S_v^*}{N_h^*} & -b\gamma_v \frac{S_v^*}{N_h^*} & -b\gamma_v \frac{S_v^*}{N_h^*} & 0 & -\mu_v & 0 \\ 0 & 0 & 0 & b\gamma_v \frac{S_v^*}{N_h^*} & b\gamma_v \frac{S_v^*}{N_h^*} & b\gamma_v \frac{S_v^*}{N_h^*} & 0 & 0 & -\mu_v \end{pmatrix}, \quad (2.3)$$

where

$D_1=\beta_p+\alpha_2+\mu_h$, $D_2=\beta_s+\mu_h$, $D_3=\alpha_1+\mu_h$, $D_4=\sigma_2+\sigma_p+\beta+\mu_p+\mu_h$,

$D_5=\sigma_c+\beta_c+\mu_c+\mu_h$, $D_6=\sigma_a+\sigma_1+\mu_a+\mu_h$,

From (2.3), it can be easily seen that $-\mu_h$ and $-\mu_v$ are eigenvalues of the Jacobian matrix. After obtaining the two eigenvalues, (2.3) reduces to

$$J_1=\begin{pmatrix} -D_1 & 0 & \alpha_1 & 0 & 0 & 0 & -b\gamma_p \frac{S_p^*}{N_h^*} \\ \beta_p & -D_2 & 0 & \beta(1-\alpha) & 0 & 0 & -b\gamma_c \frac{S_c^*}{N_h^*} \\ \alpha_2 & \beta_s & -D_3 & 0 & 0 & 0 & -b\gamma_a \frac{S_a^*}{N^*{}_h} \\ 0 & 0 & 0 & -D_4 & 0 & \sigma_1 & b\gamma_p \frac{S_p^*}{N_h^*} \\ 0 & 0 & 0 & \beta\alpha & -D_5 & 0 & b\gamma_c \frac{S_c^*}{N_h^*} \\ 0 & 0 & 0 & \sigma_2 & \beta_c & -D_6 & b\gamma_a \frac{S_a^*}{N_h^*} \\ 0 & 0 & 0 & b\gamma_v \frac{S_v^*}{N_h^*} & b\gamma_v \frac{S_v^*}{N_h^*} & b\gamma_v \frac{S_v^*}{N_h^*} & -\mu_v \end{pmatrix}. \quad (2.4)$$

The matrix (2.4) can be written as

$$J_1 = \begin{pmatrix} A & B \\ C & D \end{pmatrix}, \text{ with, } A = \begin{pmatrix} -D_1 & 0 & \alpha_1 \\ \beta_p & -D_2 & 0 \\ \alpha_2 & \beta_s & -D_3 \end{pmatrix},$$

$$B = \begin{pmatrix} 0 & 0 & 0 & -b\gamma_p \frac{S_p^*}{N_h^*} \\ \beta(1-\alpha) & 0 & 0 & -b\gamma_c \frac{S_c^*}{N_h^*} \\ 0 & 0 & 0 & -b\gamma_a \frac{S_a^*}{N_h^*} \end{pmatrix},$$

$$C = \begin{pmatrix} 0 & 0 & 0 \\ 0 & 0 & 0 \\ 0 & 0 & 0 \\ 0 & 0 & 0 \end{pmatrix} \text{ and } D = \begin{pmatrix} -D_4 & 0 & \sigma_1 & b\gamma_p \frac{S_p^*}{N_h^*} \\ \beta\alpha & -D_5 & 0 & b\gamma_c \frac{S_c^*}{N_h^*} \\ \sigma_2 & \beta_c & -D_6 & b\gamma_a \frac{S_a^*}{N_h^*} \\ b\gamma_v \frac{S_v^*}{N_h^*} & b\gamma_v \frac{S_v^*}{N_h^*} & b\gamma_v \frac{S_v^*}{N_h^*} & -\mu_v \end{pmatrix}.$$

Applying determinant of block matrices

$$\det(J_1) = \det(\mathrm{A})\det(\mathrm{D} - CA^{-1}B), \qquad (2.5)$$

since matrix C is zero, (2.5) reduces to

$$\det(J_1) = \det(A)\det(D). \qquad (2.6)$$

The corresponding characteristic polynomials of matrix A and D are given by $\lambda^3 + A_2\lambda^2 + A_1\lambda + A_0 = 0$ and $\lambda^4 + B_3\lambda^3 + B_2\lambda^2 + B_1\lambda + B_0 = 0$ respectively, where

$$A_2 = D_1 + D_2 + D_3,$$

$$A_1 = D_1D_2 + D_1D_3 + D_2D_3 - \alpha_1\alpha_2,$$

$$A_0 = D_1D_2D_3 - D_2\alpha_1\alpha_2 - \alpha_1\beta_p\beta_s,$$

$$B_3 = D_4 + D_5 + D_6 + \mu_v,$$

$$\begin{aligned} B_2 = &- \frac{b^2\gamma_a S_a^* S_v^* \gamma_v}{\left(S_c^* + S_p^* + S_a^*\right)^2} - \frac{b^2\gamma_a S_c^* S_v^* \gamma_v}{\left(S_c^* + S_p^* + S_a^*\right)^2} - \frac{b^2\gamma_a S_p^* S_v^* \gamma_v}{\left(S_c^* + S_p^* + S_a^*\right)^2} + \left(\mu_h + \mu_a + \sigma_a + \sigma_1\right)\left(\beta_c + \mu_c + \sigma_c + \mu_h\right) \\ &+ \left(\beta_c + \mu_c + \sigma_c + \mu_h\right)\left(\beta + \mu_h + \mu_p + \sigma_p + \sigma_2\right) + \mu_v\left(\beta_c + \mu_c + \sigma_c + \mu_h\right) \\ &+ \left(\mu_h + \mu_a + \sigma_a + \sigma_1\right)\left(\beta + \mu_h + \mu_p + \sigma_p + \sigma_2\right) + \mu_v\left(\beta + \mu_h + \mu_p + \sigma_p + \sigma_2\right) \\ &+ \mu_v\left(\mu_h + \mu_a + \sigma_a + \sigma_1\right) - \sigma_1\sigma_2, \end{aligned}$$

$$B_1 = -\frac{b^2\gamma_p S_p^* S_v^* \gamma_v \alpha\beta}{\left(S_c^*+S_p^*+S_a^*\right)^2} - \frac{b^2\gamma_a S_a^* S_v^* \gamma_v (\beta_c+\mu_c+\sigma_c+\mu_h)}{\left(S_c^*+S_p^*+S_a^*\right)^2} - \frac{b^2\gamma_p S_p^* S_v^* \gamma_v (\beta_c+\mu_c+\sigma_c+\mu_h)}{\left(S_c^*+S_p^*+S_a^*\right)^2} - \frac{b^2\gamma_a S_a^* S_v^* \gamma_v \left(\beta+\mu_p+\sigma_p+\sigma_2+\mu_h\right)}{\left(S_c^*+S_p^*+S_a^*\right)^2}$$

$$- \frac{b^2\gamma_p S_p^* S_v^* \gamma_v \sigma_2}{\left(S_c^*+S_p^*+S_a^*\right)^2} - \frac{b^2\gamma_c S_c^* S_v^* \gamma_v \left(\beta+\mu_p+\sigma_p+\sigma_2+\mu_h\right)}{\left(S_c^*+S_p^*+S_a^*\right)^2} - \frac{b^2\gamma_c S_c^* S_v^* \gamma_v \beta_c}{\left(S_c^*+S_p^*+S_a^*\right)^2} - \frac{b^2\gamma_a S_a^* S_v^* \gamma_v \sigma_1}{\left(S_c^*+S_p^*+S_a^*\right)^2} - \frac{b^2\gamma_c S_c^* S_v^* \gamma_v (\mu_h+\mu_a+\sigma_a+\sigma_1)}{\left(S_c^*+S_p^*+S_a^*\right)^2}$$

$$- \alpha\beta\sigma_1\beta_c - \sigma_1\sigma_2\left(\beta_c+\mu_c+\sigma_c+\mu_h\right) - \sigma_1\sigma_2\mu_v$$

$$+ \left(\mu_h+\mu_a+\sigma_a+\sigma_1\right)\left(\beta_c+\mu_c+\sigma_c+\mu_h\right)\left(\beta+\mu_p+\sigma_p+\sigma_2+\mu_h\right)$$

$$+ \mu_v\left(\beta_c+\mu_c+\sigma_c+\mu_h\right)\left(\beta+\mu_p+\sigma_p+\sigma_2+\mu_h\right)$$

$$+ \mu_v\left(\mu_h+\mu_a+\sigma_a+\sigma_1\right)\left(\beta_c+\mu_c+\sigma_c+\mu_h\right)$$

$$+ \mu_v\left(\mu_h+\mu_a+\sigma_a+\sigma_1\right)\left(\beta+\mu_p+\sigma_p+\sigma_2+\mu_h\right),$$

$$B_0 = -\frac{b^2\gamma_a S_a^* S_v^* \gamma_v \alpha\beta\sigma_1}{\left(S_c^*+S_p^*+S_a^*\right)^2} - \frac{b^2\gamma_a S_a^* S_v^* \gamma_v \sigma_1 (\beta_c+\mu_c+\sigma_c+\mu_h)}{\left(S_c^*+S_p^*+S_a^*\right)^2} - \frac{b^2\gamma_p S_p^* S_v^* \gamma_v \sigma_2 (\beta_c+\mu_c+\sigma_c+\mu_h)}{\left(S_c^*+S_p^*+S_a^*\right)^2} - \frac{b^2\gamma_c S_c^* S_v^* \gamma_v \beta_c \left(\beta+\mu_p+\sigma_p+\sigma_2+\mu_h\right)}{\left(S_c^*+S_p^*+S_a^*\right)^2}$$

$$- \frac{b^2\gamma_p S_p^* S_v^* \gamma_v \alpha\beta\beta_c}{\left(S_c^*+S_p^*+S_a^*\right)^2} - \frac{b^2\gamma_c S_c^* S_v^* \gamma_v (\mu_h+\mu_a+\sigma_a+\sigma_1)\left(\beta+\mu_p+\sigma_p+\sigma_2+\mu_h\right)}{\left(S_c^*+S_p^*+S_a^*\right)^2} - \frac{b^2\gamma_c S_c^* S_v^* \gamma_v \sigma_1\beta_c}{\left(S_c^*+S_p^*+S_a^*\right)^2} - \frac{b^2\gamma_c S_c^* S_v^* \gamma_v \sigma_1\sigma_2}{\left(S_c^*+S_p^*+S_a^*\right)^2}$$

$$- \frac{b^2\gamma_p S_p^* S_v^* \gamma_v (\mu_h+\mu_a+\sigma_a+\sigma_1)}{\left(S_c^*+S_p^*+S_a^*\right)^2} - \frac{b^2\gamma_p S_p^* S_v^* \gamma_v (\mu_h+\mu_a+\sigma_a+\sigma_1)(\beta_c+\mu_c+\sigma_c+\mu_h)}{\left(S_c^*+S_p^*+S_a^*\right)^2}$$

$$- \frac{b^2\gamma_a S_a^* S_v^* \gamma_v (\beta_c+\mu_c+\sigma_c+\mu_h)\left(\beta+\mu_p+\sigma_p+\sigma_2+\mu_h\right)}{\left(S_c^*+S_p^*+S_a^*\right)^2} - \alpha\beta\sigma_1\beta_c\mu_v - \sigma_1\sigma_2\mu_v\left(\beta_c+\mu_c+\sigma_c+\mu_h\right)$$

$$+ \mu_v\left(\mu_h+\mu_a+\sigma_a+\sigma_1\right)\left(\beta_c+\mu_c+\sigma_c+\mu_h\right)\left(\beta+\mu_p+\sigma_p+\sigma_2+\mu_h\right).$$

Therefore, by Routh array, we obtain the tables below whereby first and second rows are filled using the coefficients of the given characteristic polynomials and the remaining rows are filled with corresponding determinants.

$$\lambda^3 + A_2\lambda^2 + A_1\lambda + A_0 = 0,$$

λ^3	1	A_1	0
λ^2	A_2	A_0	0
λ^1	w_1	0	
λ^0	A_0		

and

$$\lambda^4 + B_3\lambda^3 + B_2\lambda^2 + B_1\lambda + B_0 = 0.$$

λ^4	1	B_2	B_0
λ^3	B_3	B_1	0
λ^2	w_2	B_0	
λ^1	w_3	0	
λ^0	B_0		

For the model system to be stable, values in the first column of the tables obtained above must be all non-neagative. So, using the Mathematica package, it is observed that, $A_2 > 0$, $w_1 = \frac{A_1 A_2 - A_0}{A_2} > 0$ and $A_0 > 0$. Moreover, $B_3 > 0$, and $w_2 = \frac{B_3 B_2 - B_1}{B_3}$, $w_3 = \frac{B_3 B_2 B_1 - B_1^2 - B_3^2 B_0}{B_3 B_2 - B_1}$ and B_0 are positive if $R_0 < 1$. Therefore, the disease-free equilibrium is locally asymptotically stable. #

Global Stability of the Disease-Free Equilibrium

In this sub-section, we want to show that the Disease-free equilibrium will be globally asymptotically stable if $R_0 < 1$, by analyzing the condition for global stability of the disease-free equilibrium of the model. The theorem by Castillo-Chavez (2002) is used to analyze the global stability of the disease-free equilibrium. From the theorem, the model system (2.1) can be written as:

$$\begin{aligned} \frac{dX_1}{dt} &= Y_1(X_1, X_2), \\ \frac{dX_2}{dt} &= Y_2(X_1, X_2), Y_2(X_1, 0) = 0. \end{aligned} \tag{2.7}$$

Where $X_1 \in R_+^5$ is a column-vector comprises of uninfected compartments, and $X_2 \in R_+^4$ consists of infected compartments. $E_0 = \left(X_1^*, 0\right)$ is the disease-free equilibrium of (2.1), and is globally asymptotically stable for $R_0 < 1$, and if it satisfies the following assumptions.

$K_1 : \frac{dX_1}{dt} = Y_1\left(X_1, 0\right)$, X_1^* is globally asymptotically stable, and $Y_1\left(X_1, 0\right)$ is the disease-free of model equations (2.1).

$K_2 : Y_2(X_1, X_2) = MX_2 - \bar{Y}_2(X_1, X_2)$, $\bar{Y}_2(X_1, X_2) \geq 0$ for $(X_1, X_2) \in \Omega_{Y_1}$.

$M = \frac{\partial Y_2}{\partial X_2}\left(X_1^*, 0\right)$ is a Metzler-matrix with non-negative off diagonal elements.

$X_1 = \left(S_p, S_c, S_a, R_h, S_v\right)$ and $X_2 = (I_p, I_c, I_a, I_v)$.

Theorem 2. *The disease-free equilibrium of the model (2.1) is a globally asymptotically stable if* $R_0 < 1$, *and satisfies the conditions* K_1 *and* K_2.

Proof:

Consider the model system (2.1)

$$Y_1(X_1, 0) = \begin{pmatrix} \alpha_1 S_a - (\beta_p + \alpha_2 + \mu_h) S_p \\ \beta_p S_p - (\beta_s + \mu_h) S_c \\ \pi_a + \beta_s S_c + \alpha_2 S_p - (\alpha_1 + \mu_h) S_a \\ \eta(T, R_m) - \mu_v S_v \end{pmatrix}, \tag{2.8}$$

$Y_2(X_1, X_2) = MX_2 - \bar{Y}_2(X_1, X_2)$, but

$$Y_2(X_1, X_2) = \begin{pmatrix} b\gamma_p I_v \frac{S_p}{N_h} + \sigma_1 I_a - D_4 I_p \\ b\gamma_c I_v \frac{S_c}{N_h} + \beta\alpha I_p - D_5 I_c \\ b\gamma_a I_v \frac{S_a}{N_h} + \sigma_2 I_p + \beta_c I_c - D_6 I_a \\ b\gamma_v S_v \frac{I_p}{N_h} + b\gamma_v S_v \frac{I_c}{N_h} + b\gamma_v S_v \frac{I_a}{N_h} - \mu_v I_v \end{pmatrix}$$

and

$$M = \begin{pmatrix} -D_4 & 0 & \sigma_1 & b\gamma_p \frac{S_p^*}{N_h^*} \\ \beta\alpha & -D_5 & 0 & b\gamma_c \frac{S_c^*}{N_h^*} \\ \sigma_2 & \beta_c & -D_6 & b\gamma_a \frac{S_a^*}{N_h^*} \\ b\gamma_v \frac{S_v^*}{N_h^*} & b\gamma_v \frac{S_v^*}{N_h^*} & b\gamma_v \frac{S_v^*}{N_h^*} & -\mu_v \end{pmatrix}.$$

Hence, $\bar{Y}_2(X_1, X_2) = \begin{pmatrix} 0 \\ 0 \\ 0 \\ 0 \end{pmatrix}$. (2.9)

Since matrix (2.8) satisfies the disease-free of model system (2.1), then the condition K_1 is met and from matrix (2.9), the condition K_2 is also satisfied. Therefore, the disease-free equilibrium E_0 is globally asymptotically stable. #

Existence of Endemic Equilibrium

The model system (2.1) has at least one possible unique endemic equilibrium point $E^*(S_p^*, S_c^*, S_a^*, I_p^*, I_c^*, I_a^*, R_h^*, S_v^*, I_v^*)$ if $R_0 < 1$ and must satisfy

$$S_p^* = \frac{\alpha_1 S_a^*}{\lambda_p + \beta_p + \alpha_2 + \mu_h},\ S_c^* = \frac{\beta(1-\alpha) I_p^* + \beta_p S_p^*}{\lambda_c + \beta_s + \mu_h},\quad S_a^* = \frac{\pi_a + \beta_s S_p^* + \alpha_2 S_p^*}{\lambda_a + \alpha_1 + \mu_h},\quad I_p^* = \frac{\lambda_p S_p^* + \sigma_1 I_a^*}{\sigma_2 + \sigma_p + \beta + \mu_p + \mu_h}$$

$$I_c^* = \frac{\lambda_p S_c^* + \beta\alpha I_p^*}{\sigma_c + \beta_c + \mu_c + \mu_h},\quad I_a^* = \frac{\lambda_a S_a + \alpha_2 I_p^* + \beta_c I_p^*}{\sigma_1 + \sigma_2 + \mu_a + \mu_h},\quad R_h^* = \frac{\sigma_p I_p^* + \sigma_c I_p^* + \sigma_a I_p^*}{\mu_h},\quad S_v^* = \frac{\eta(T, R_m)}{\lambda_v + \mu_v},\ (2.10)$$

$$I_v^* = \frac{\lambda_v \eta(T, R_m)}{(\lambda_v + \mu_v)\mu_v}.$$

The solutions in (2.10) are too complex to show the existence and nature of the endemic equilibrium explicitly. However, at endemic I_p^*, I_c^*, I_a^* and I_v^* are all greater than zero, hence the endemic equilibrium exists.

Global Stability of the Endemic Equilibrium

This section presents global stability of the endemic equilibrium of model system (2.1) using the Lyapunov function.

Theorem 3. *The endemic equilibrium of the model system (2.1) is globally asymptotically stable if* $R_0 > 1$ *and unstable otherwise.*

Proof:

We consider the Lyapunov function basing on the composite quadratic function as used by Vargas-De-Le´on (2009).

$$W = \tfrac{1}{2}\left[\left(S_p - S_p^*\right)+\left(S_c - S_c^*\right)+\left(S_a - S_a^*\right)+\left(I_p - I_p^*\right)+\left(I_c - I_c^*\right)+\left(I_a - I_a^*\right)+\left(R_h - R_h^*\right)\right]^2 + \tfrac{1}{2}\left[\left(S_v - S_v^*\right)+\left(I_v - I_v^*\right)\right]^2$$

$$\frac{dW}{dt} = \left[\left(S_p - S_p^*\right)+\left(S_c - S_c^*\right)+\left(S_a - S_a^*\right)+\left(I_p - I_p^*\right)+\left(I_c - I_c^*\right)+\left(I_a - I_a^*\right)+\left(R_h - R_h^*\right)\right] \times \frac{d}{dt}\left(S_p + S_c + S_a + I_p + I_c + I_a + R_h\right)+\left[\left(S_v - S_v^*\right)+\left(I_v - I_v^*\right)\right]\times \frac{d}{dt}\left(S_v + I_v\right).$$

(2.11)

Substituting model system (2.1) into equation (2.11) gives

$$\frac{dW}{dt} = \left[\left(S_p - S_p^*\right)+\left(S_c - S_c^*\right)+\left(S_a - S_a^*\right)+\left(I_p - I_p^*\right)+\left(I_c - I_c^*\right)+\left(I_a - I_a^*\right)+\left(R_h - R_h^*\right)\right] \times\left[\pi_a - \mu_h\left(S_p + S_c + S_a + I_p + I_c + I_a + R_h\right) - \mu_p I_p - \mu_c I_c - \mu_a I_a\right] +\left[\left(S_v - S_v^*\right)+\left(I_v - I_v^*\right)\right]\times\left[\eta(T, R_m) - \mu_v\left(S_v + I_v\right)\right].$$

(2.12)

Applying $\pi_a = \mu_h(S_p^* + S_c^* + S_a^* + I_p^* + I_c^* + I_a^* + R_h^*)$ and $\eta(T, R_m) = \mu_v(S_v^* + I_v^*)$ into (2.12) yields,

$$\frac{dW}{dt} = -\mu_h\left[\left(S_p - S_p^*\right)+\left(S_c - S_c^*\right)+\left(S_a - S_a^*\right)+\left(R_h - R_h^*\right)\right]^2 -\left[(\mu_p + \mu_h)(I_p - I_p^*)^2 + (\mu_c + \mu_h)(I_c - I_p^*)^2 + (\mu_a + \mu_h)(I_a - I_p^*)^2\right] - \mu_v\left[\left(S_v - S_v^*\right)+\left(I_v - I_v^*\right)\right]^2. \quad (2.13)$$

From equation (2.13), it is observed that $\frac{dW}{dt} < 0$ in $\left\{S_p, S_c, S_a, I_p, I_c, I_a, R_h, S_v, I_v\right\} \in \Omega$ and the condition $\frac{dW}{dt} = 0$ holds if

$$\left(S_p, S_c, S_a, I_p, I_c, I_a, R_h, S_v, I_v\right) = \left(S_p^*, S_c^*, S_a^*, I_p^*, I_c^*, I_a^*, R_h^*, S_v^*, I_v^*\right).$$

Hence, by LaSalle's invariant principle (LaSalle 1976), the endemic equilibrium of model system (2.1) is globally asymptotically stable.

Temperature and Rainfall Dependent Variables

In this subsection, temperature and rainfall variables incorporated in model system (2.1) are defined. It is assumed that, mosquito recruitment rate $\eta(T, R_m)$ depends on temperature and rainfall. According to Yiga et al. (2020) mosquito natural death rate is defined by $\mu_v(T) = -\ln\left(0.522 - 0.000828T^2 + 0.0367T\right)$ and the study by Ngarakana-Gwasira et al. (2016) expressed mosquito birth rate as

$$\eta(T,R_m)=\frac{n_e\rho_e(R_m)\rho_l(T,R_m)\rho_p(R_m)}{d_e+d_l(T)+d_p}, \quad (2.14)$$

with

$$\rho_l(T,R_m)=\frac{4\rho_m}{R_l^2}(R_mR_l-R_m^2)e^{-(0.00554T+0.06757)}, \quad (2.15)$$

$$\rho_e(R_m)=\rho_p(R_m)=\frac{4\rho_m}{R_l^2}(R_mR_l-R_m^2), \quad (2.16)$$

$$d_l(T)=(0.00554T-0.06757)^{-1}, \quad (2.17)$$

$$\rho_m=0.9,0.25,0.75, \quad (2.18)$$

$$d_e=1\text{Month}, \quad (2.19)$$

$$d_p=1\text{Month} \quad (2.20)$$

and

$$n_e=6000. \quad (2.21)$$

where, n_e is the number of eggs a mosquito can lay per month, R_l is the threshold rainfall beyond which there is no survival for immature mosquitoes as it is noted that excessive rainfall may flush out breading sites. Moreover, $\rho_m(m=e,l,p)$ is the maximum survival probability at optimum rainfall for mosquito breeding, while $\rho_e(R_m)$, $\rho_l(T,R_m)$ and $\rho_p(R_m)$ are survival probabilities for eggs, larvae and pupae respectively. Further, d_e, $d_l(T)$ and d_p are corresponding development duration for each stage. Substituting (2.15), (2.16), (2.17), (2.18), (2.19), (2.20) and (2.21) into (2.14) gives adult mosquitoes recruited per month. That is,

$$\eta(T,R_m)=\frac{(33.24T-405.42)\left(R_mR_l-R_m^2\right)^3e^{-0.00554T-0.067}}{R_l^6(0.01108T+0.86486)}$$

. Following the work by Parham and Michael (2010), the mosquito-biting rate is expressed by $b(T)=\frac{T-T_{\min}}{D}$. Where, $T_{\min}$ is the minimum temperature that favors mosquito biting, and D is the number of days in which temperature was favorable for mosquito activities, known as degree days.

Numerical Results and Discussion

In this section, model (2.1) involving temperature dependent parameter $\mu_v(T)$ and temperature and rainfall dependent parameter $\eta(T,R_m)$ is solved numerically by using Runge-Kutta technique. The values of these parameters are obtained numerically using their corresponding formulas as described in the section of temperature and rainfall dependent variables. The aim is to validate the analytical solutions obtained in the previous sections. The implementation of the method/scheme was done using MATLAB package. Plots of numerical solutions are used to investigate the effects of temperature and rainfall on dynamics of malaria transmission in the structured population of pregnant women, children up to five years and individuals above five years old. The parameters used for simulation are as shown in Table 1, while the initial values for the subpopulations are given as follows:

$S_p=40$, $S_c=120$, $S_a=60$

$I_p=8$, $I_c=25$, $I_a=20$,

$R_h=30$, $S_v=80000$ and

$I_v=5000.$

Table 1: Parameter Description and Values

Parameter	Description	Value (Month^{-1})	Source
π_a	Recruitment rate in S_a	0.028	Ngarakana-Gwasira et al. (2016)
μ_h	Human natural death rate	0.019	Traor´e et al. (2017)
μ_p	Induced death rate in I_p	0.49273	Azu-Tungmah et al. (2019)
μ_c	Induced death rate in I_c	0.50605	Assumed
μ_a	Induced death rate in I_a	0.0028	Traor´e et al. (2017)
σ_p	Recovery rate in I_p	0.14154	Azu-Tungmah et al. (2019)
σ_c	Recovery rate in I_c	0.07 (0025/Day)	Gumel and Okuneye (2017)
σ_a	Recovery rate in I_a	0.0159	Traor´e et al. (2017)
γ_p	Infection rate in S_p	0.32150	Assumed
γ_c	Infection rate in S_c	0.33575	Azu-Tungmah et al. (2019)
γ_a	Infection rate in S_a	0.16246	Kalula et al. (2023)
γ_v	Infection rate in S_v	0.616(0.022/Day)	Gumel and Okuneye (2017)
σ_1	The rate at which individual from I_a move to I_p	0.016744	Azu-Tungmah et al. (2019)
σ_2	The rate at which individual from I_p move to I_a	0.691	Ou´edraogo et al. (2012)
β_s	Progression rate from S_c into S_a	0.00092732	Kalula et al. (2023)
β_c	Progression rate from I_c to I_a	0.00092732	Kalula et al. (2023)
β_p	Delivery rate of babies in S_p	0.691	Ou´edraogo et al. (2012)
β	Delivery rate of babies in I_p	0.691	Ou´edraogo et al. (2012)
α	Proportion of babies born with infections	0.0549	Ou´edraogo et al. (2012)
α_1	The rate at which individuals from S_a move to S_p after conceiving	0.094735852	Assumed
α_2	The rate at which individuals	0.20232	Assumed

	from S_p move to S_a after delivery		
R_l	Threshold rainfall beyond which no survival of immature mosquito	50	Ngarakana-Gwasira et al. (2016)
D	Temperature days	111	Parham and Michael (2010)
$T_{\min}$	Minimum temperature	16	Parham and Michael (2010)

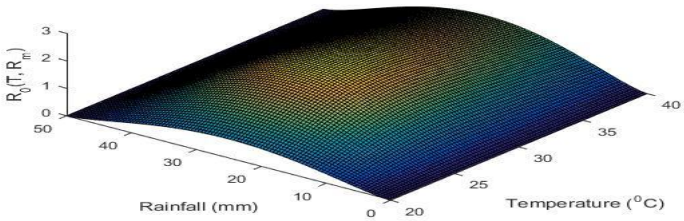

Figure 2: The impact of Temperature and Rainfall on R_0

From Figure 2, it is observed that malaria transmission occurs at temperature between (20 ^0C −40 ^0C) and rainfall range (0−50 mm), and the optimal temperature and rainfall are 28.94^0C and 26.88 mm respectively. Moreover, the result indicates that $R_0 > 1$ at temperature and rainfall ranging between (23.53 ^0C − 39.80 ^0C) and (14.82 mm − 38.44 mm) respectively. The temperature range at which malaria transmission occurs is similar to the findings of (Ngarakana-Gwasira et al. (2016), Parham and Michael (2010)) which are (20 ^0C – 40 ^0C) and (20 ^0C – 39 ^0C). Furthermore, the temperature range at which $R_0 > 1$ and the optimal temperature correspond to the results by Abiodun et al. (2018) which are (18 ^0C −38 ^0C) and 30 ^0C respectively. The rainfall range is in line with Ngarakana-Gwasira et al. (2016), Yiga et al. (2020) which is 0 – 50 mm, and the optimal rainfall is closer to the result by Yiga et al. (2020) which is 30 mm.

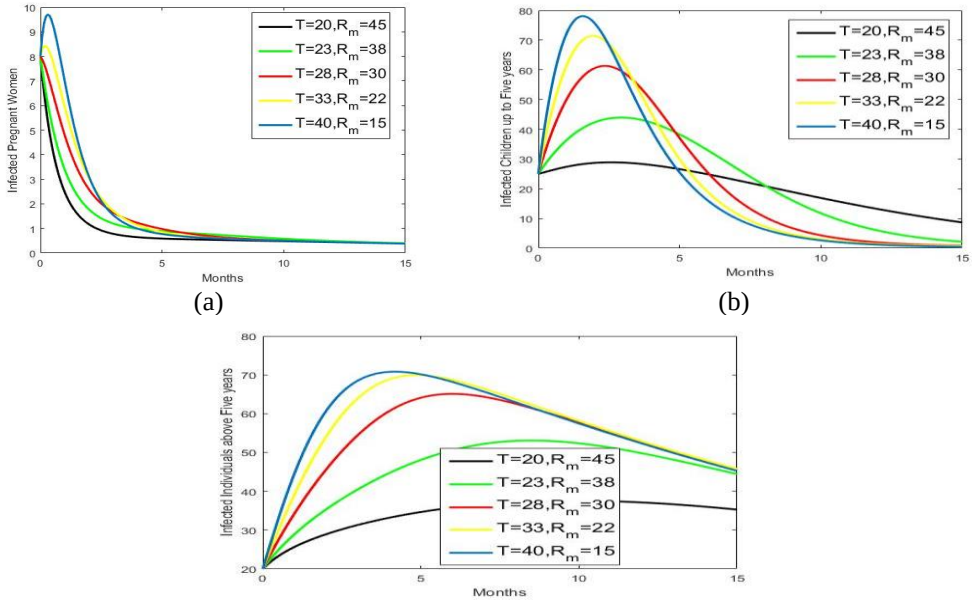

Figure 3: The impact of Temperature and Rainfall on Malaria Infections in (a) Pregnant women, (b) Children up to five years and (c) Individuals above five years.

From Figure 3, it is observed that, the lowest number of infected individuals occurs at temperature $T = 20\ ^0C$ and rainfall $R_m = 45$ mm. These results are due to the fact that malaria infections increase ($R_0 > 1$) with increasing temperature and decreasing rainfall or vice versa. Moreover, the results show a rapid increase of infections in pregnant women and children up to five years. The rapid increase of infections in the two groups is due to the weak immunity as compared to individuals above five years. Furthermore, the infections drop down as time goes on due to deaths and recovery. These results agree with that by Yiga et al. (2020).

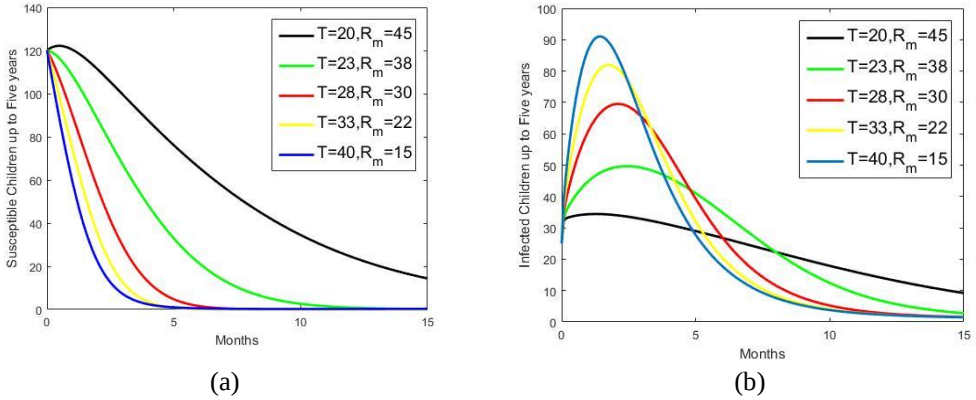

Figure 4: The effects of transplacental transmission when $\alpha = 1$ on (a) susceptible Children up to five years and (b) Infected children up to five years.

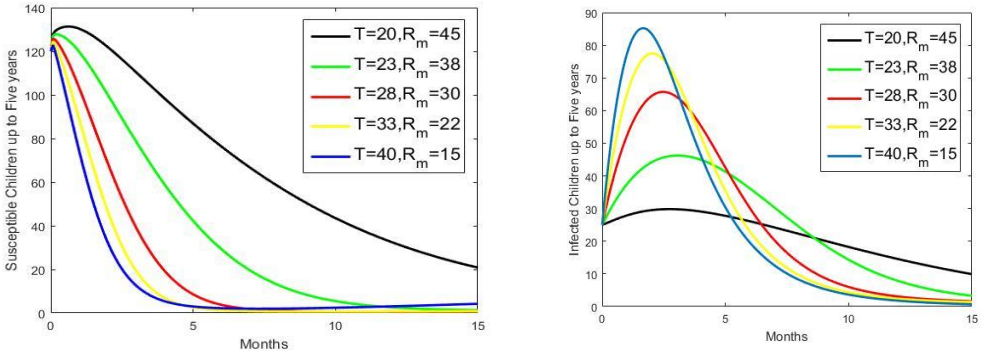

(a) (b)

Figure 5: The effects of transplacental transmission when $\alpha = 0$ on (a) susceptible Children up to five years and (b) Infected children up to five years.

The numerical simulation for Figures 4 and 5 was carried out using $I_p = 30$. So, it was expected at least 30 babies to be born from infected pregnant women. We assumed that among these babies, some were born with infections. From the result in Figures 4 and 5, it is observed that decreasing the rate of transplacental transmission, α from 1 to 0, increases the number of individuals born free of malaria.

Sensitivity Analysis

Sensitivity analysis explains how parameters of the model system contribute to the model output. There are two major ways of performing sensitivity analysis, that is local and global sensitivity analyses. This sub-section performs local sensitivity analysis.

Local sensitivity analysis determines how each of the parameters affects the reproduction number R_0 as the model output. In this approach only one parameter is varied and fix the others. We compute sensitivity indices of R_0 with respect to a parameter(s) using the forward normalized sensitive index of a variable as applied by Chitnis et al. (2008). That is if ℓ is a variable, w is a parameter and r is the reproduction number then the sensitivity index of a variable ℓ is given as: $\ell_r^w = \frac{\partial r}{\partial w} \times \frac{w}{r}$. The sensitivity indices are generated using parameter values in Table 1 and presented in Table 2. The numerical result for the local sensitivity is shown in Figure 6.

Table 2: Sensitivity indices

Parameter	Sensitivity index	Parameter	Sensitivity index
$b(T)$	1	π_a	-0.5
μ_h	-0.542	γ_c	0.554
μ_p	-0.0204	γ_a	0.048
μ_c	-0.426	γ_v	0.500
μ_a	-0.00347	σ_1	-0.00105
σ_p	-0.000367	σ_2	0.000085

σ_c	-0.0156	β_c	0.0014
σ_a	-0.0153	β	-0.0038
γ_p	0.255	α	-0.069
$\eta(T,R_m)$	0.5	$\mu_v(T)$	-1

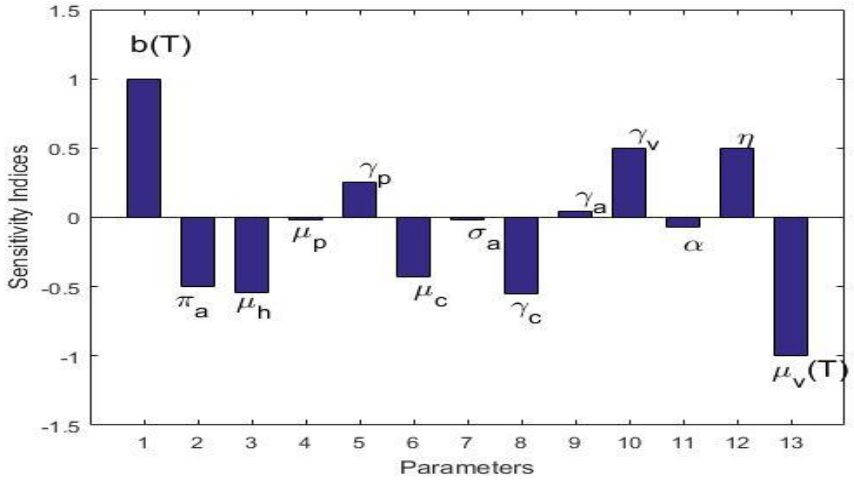

Figure 6: Numerical local sensitivity analysis of most sensitive parameters on R_0

From Table 2, the parameters, ($b(T)$, $\eta(T,R_m)$, γ_p , γ_c , γ_a , γ_v , σ_2 , β_c) are all positive and (π_a , μ_h , μ_p , μ_c , μ_a , $\mu_v(T)$, σ_1 , σ_a , σ_p , σ_c) are all negative. The positive sensitivity index indicates that the parameter is directly proportional to the reproduction number while the negative sensitivity index shows that the parameter is inversely proportional to the reproduction number. That is, increasing or decreasing one of these positive parameters cause the increase or decrease of the reproduction number while increasing or decreasing one of the negative parameters lead to decrease or increase of the reproduction number. The magnitude of the sensitivity index indicates how R_0 is sensitive to the parameter. That is, the bigger the sensitivity index the more sensitive the reproduction number is, to the parameter and vice versa. For instance, the results in Table 2 and Figure 6 show that biting rate $b(T)$ is the most sensitive parameter since it has the highest positive value, which is, +1. This outcome is in line with the previous studies conducted by Chitnis et al. (2008) and Kalula et al. (2021). This result implies that, increasing or decreasing mosquito-biting rate, results into increase or decrease of malaria infections of malaria by exactly the same amount. Natural death rate of mosquitoes is another more sensitive parameter. It has the highest negative value that is, -1. Thus, increasing or decreasing death of mosquitoes will result into decrease or increase of malaria infections by exactly the same number. The results indicate that the next parameters with great effects are (η , π_a γ_c , γ_v , μ_h , μ_c , γ_p , μ_p α , σ_a γ_a).

Conclusion

The aim of this study was to investigate the effects of temperature and rainfall on the transmission dynamics of malaria in an age-structured population. This was done by formulating a mathematical model for malaria using ordinary differential equations.

The numerical results show that at temperature and rainfall ranges between ($23.53\ 0C - 39.80\ ^0C$) and (14.82 mm − 38.44 mm) respectively, there are high rates of malaria infections especially to pregnant women and children up to five years. Moreover, decreasing the rate of transplacental transmission increases the number of children born without infections. Thus, in order to minimize malaria transmission, human individuals should be aware of the variations of temperature, rainfall, and their corresponding ranges at which malaria transmission occurs most, so that they can take precautions.

Acknowledgements

Authors are grateful for support from the University of Dar es Salaam.

Declaration

The authors declare that there is no conflict of interest.

References

Abiodun GJ, Witbooi P and Okosun KO 2018 Modelling the impact of climatic variables on malaria transmission. *Hacet. J. Math. Stat.* 47(2):219–235.

Azu-Tungmah GT, Oduro FT and Okyere G A 2019 Optimal control analysis of an age-structured malaria model incorporating children under five years and pregnant women. *J. Adv. Math. Comput*. 30(6):1–23.

Bakare E and Abolarin O 2018 Optimal control of malaria transmission dynamics with seasonality in rainfall. *Int. J. Pure Appl. Math*. 119(3):519–539.

Bakary T, Boureima S and Sado T 2018 A mathematical model of malaria transmission in a periodic environment. *J. Biol. Dyn*. 12(1):400–432.

Blanford JI, Blanford S, Crane RG, Mann ME, Paaijmans KP, Schreiber KV and Thomas MB 2013 Implications of temperature variation for malaria parasite development across africa. *Sci. Rep*. 3:1300 https://doi.org/10.1038/srep01300.

Castillo-Chavez C 2002 On the computation of r. and its role on global stability. *Sci. Res.* 125:229-250.

Chitnis N, Hyman JM and Cushing JM 2008 Determining important parameters in the spread of malaria through the sensitivity analysis of a mathematical model. *Bull. Math. Biol.* 70:1272–1296.

Gumel AB and Okuneye K 2017 Analysis of a temperature and rainfall dependent model for malaria transmission dynamics. *Math. Biosci.* 287:72-92.

Kalula A, Mureithi E, Marijani T and Mbalawata I 2023 Optimal control and cost-effectiveness analysis of age-structured malaria model with asymptomatic carrier and temperature variability. *J. Biol. Dyn.* 17(1):1-35.

Kalula AS, Mureithi E, Marijani T and Mbalawata I 2021 An age-structured model for transmission dynamics of malaria with infected immigrants and asymptomatic carriers. *Tanz. J. Sci.* 47(3):953–968.

Kipkirui M, Kirui W and Adicka D 2020 Modelling of malaria transmission using delay differential equation. *Math. Model. Appl.* 5(3):167-175.

Kumar STPRCP and Reddy N 2014 Factors affecting malaria disease transmission and incidence: a special focus on Visakhapatnam district. *Int. J. Sci. Res*. 5(1):312–317.

LaSalle J P 1976 The Stability of Dynamical Systems. *SIAM.* 1976: 57-76

Mwaiswelo RO, Mmbando BP, Chacky F, Molteni F, Mohamed A, Lazaro S, Mkalla,SF, Samuel B and Ngasala, B 2021 Malaria infection and anemia status in under-five children from southern Tanzania where seasonal malaria chemoprevention is being implemented. *PLoS. One*. 16(12): 1-16.

Ngarakana-Gwasira ET, Bhunu CP, Masocha M and Mashonjowa E2016 Assessing the role of climate change in malaria transmission in Africa. *Malar. Res. Treat.* 2016:1-7.

Ou´edraogo A, Tiono AB, Diarra A, Bougouma ECC, N´ebi´e I, Konat´e AT, Sirima SB 2012 Transplacental

transmission of plasmodium falciparum in a highly malaria endemic area of burkina faso. *J. Trop. Med.* 2012:1-7.

Parham PE and Michael E 2010 Modelling climate change and malaria transmission. *Adv. Exp. Med. Biol*, 673: 184–199.

Schumacher RF and Spinelli E 2012 Malaria in children. *Mediterr. J. Hematol.* 4(1): 1-12.

Traor´e B, Sangar´e B, Traor´e S 2017 A mathematical model of malaria transmission with structured vector population and seasonality. *J. Appl. Math.* 2017:1-15.

Uneke CJ 2011 Congenital malaria: an overview. *TJHR.* 13(3):264–280.

Van den Driessche P and Watmough J 2002 Reproduction numbers and sub-threshold endemic equilibria for compartmental models of disease transmission. *Math. Biosci.* 180(1-2):29–48.

Vargas-De-Le´on C 2009 Constructions of lyapunov functions for classic sis, sir and sirs epidemic models with variable population size. *Foro-Red-Mat Rev. Electron. Content. Math.* 26(5):1–12.

WHO (World Health Organization). World malaria report 2022.

WHO (World Health Organization). World malaria report 2023.

Yang HM 2000 Malaria transmission model for different levels of acquired immunity and temperature-dependent parameters (vector). *Rev. Saude Publica.* 34(3):223–231.

Yiga V, Nampala H and Tumwiine J 2020 Analysis of the model on the effect of seasonal factors on malaria transmission dynamics. *J. Appl. Math.* 2020:1–19.